Directed Self-Assembly to Create Molecular Terraces with Molecularly Sharp Boundaries in Organic Monolayers

L. A. Bumm,[†] J. J. Arnold,[†] L. F. Charles,[†] T. D. Dunbar,[‡] D. L. Allara,*,[§] and P. S. Weiss*,[†]

Contribution from the Departments of Chemistry and Materials Science and Engineering, The Pennsylvania State University, University Park, Pennsylvania 16802-6300

Received June 22, 1998. Revised Manuscript Received June 15, 1999

Abstract: We demonstrate the ability to control the placement of molecules within self-assembled films. We show quasi-two-dimensional mosaic structures within two-component self-assembled monolayers. These demonstrate new types of monolayer features: the domains of each component form molecular terraces, and the boundaries between these domains form molecular step edges. We find the molecular step edges are molecularly sharp and laterally epitaxial. The molecular step edges have the unique ability to expose a typically buried part of the larger molecule at the boundary. For the identical components in the crystalline monolayer, we can also distribute the molecules randomly. These structures were selected and created using simple controlled sequences of self-assembly and processing with different length alkanethiols on Au{111}. We have imaged these films using molecular resolution scanning tunneling microscopy.

Introduction

Deterministic control of the two-dimensional organization of adsorbed films at the molecular level will be critical for proposed future applications ranging from bio-specific surfaces[1] to molecular electronic devices[2-7] for which the placement of molecules in specific spatial arrangements is required. Manipulation of single atoms and molecules has been demonstrated.[8,9] With enough effort, complex structures could, in principle, be created on a surface. Regrettably the forces holding together these assemblies are typically weak, so the experiments must be done at low temperature[8] or with specially selected components.[9] For practical applications these molecular-scale structures must be stable at room temperature, although they need not be utilized there. In this paper we describe the synthesis and stability of sharply defined room temperature molecular mosaic structures created by directed self-assembly.

We have used the molecular resolution capability of scanning tunneling microscopy (STM) to distinguish between regions of different chemical functionality in self-assembled monolayers (SAMs) of alkanethiols on Au{111}. Surfaces can be produced with mixed ω-functionality at the exposed interface.[10-14] Despite the volume of STM work, questions remain as to the imaging mechanism and whether STM can image the exposed (alkane-thiolate-air) SAM interface.[15] To answer these questions, we probe the limit for which STM can detect small differences in two-component SAMs. To eliminate any specific chemical effects which might cause STM contrast, we chose two alkanethiols with slightly different alkyl chain length, 1-decanethiol, $CH_3(CH_2)_9SH$, and 1-dodecanethiol, $CH_3(CH_2)_{11}SH$. The difference in film thickness between the 10-carbon 1-decanethiolate (**10**) and the 12-carbon 1-dodecanethiolate (**12**) SAM is 2.2 Å for an alkyl chain tilt angle of 30°. (The difference in film thickness of 2.2 Å was calculated using the following structural factors: C–C bond distance, 1.53 Å;[16] C–C–C bond angle, 112°;[17] and the chain tilt angle, 30°.[18] This compares to ~2.2–2.4 Å obtained from ellipsometry.[18,19] Chain twist does not affect this value when the lengths differ by an *even* number of methylene units. Both molecules also adopt identical chain

* To whom correspondence should be addressed.
† Department of Chemistry.
‡ Present address: Advanced Materials Lab, Sandia National Laboratories, Albuquerque, NM 87106.
§ Departments of Chemistry and Materials Science and Engineering.
(1) Allara, D. L. *Biosens. Bioelectron.* **1995**, *10*, 771–783.
(2) Petty, M. C., Bryce, M. R., Bloor, D., Eds. *An Introduction to Molecular Electronics*; Oxford University Press: New York, 1995.
(3) Aviram, A., Ed. *Molecular Electronics: Science and Technology*, *Conference Proceedings No. 262*; American Institute of Physics: New York, 1992.
(4) Reed, M. A., Kirk, W. P., Eds. *Nanostructure Physics and Fabrication*; Academic Press: New York, 1989.
(5) Reed, M. A., Kirk, W. P., Eds. *Nanostructures and Mesoscopic Systems*; Academic Press: New York, 1992.
(6) Carter, F. L., Ed. *Molecular Electronic Devices II*; Marcel Dekker: New York, 1987.
(7) Miller, J. S. *Adv. Mater.* **1990**, *2*, 378–379, 495–497, 601–603.
(8) Eigler, D. M.; Schweizer, E. K. *Nature* **1990**, *344*, 524–526. Eigler, D. M.; Stroscio, J. A. *Science* **1991**, *254*, 1319–1325. Weiss, P. S.; Eigler, D. M. In *Nanosources and Manipulations of Atoms Under High Fields and Temperatures: Applications, NATO ASI Series E*; Binh, V. T., Garcia, N., Dransfeld, K., Eds.; Kluwer Academic Publishers: Dordrecht, The Netherlands, 1993; Vol. 235, pp 213-217.
(9) Jung, T. A.; Schlittler, R. R.; Gimzewski, J. K.; Tang, H.; Joachim, C. *Science* **1996**, *271*, 181–184.

(10) Stranick, S. J.; Parikh, A. N.; Tao, Y.-T.; Allara, D. L.; Weiss, P. S. *J. Phys. Chem.* **1994**, *98*, 8, 7636–7646.
(11) Delamarche, E.; Michel, B. *Thin Solid Films* **1996**, *273*, 54–60.
(12) Hobara, D.; Ota, M.; Imabayashi, S.-I.; Niki, K.; Kakiuchi, T. *J. Electroanal. Chem.* **1998**, *444*, 113–119.
(13) Mizutani, W.; Ishida, T.; Yamamoto, S.-I.; Tokumoto, H.; Hokari, H.; Azehara, H.; Fujihara, M. *Appl. Phys. A* **1998**, *66*, S1257–S1260.
(14) Poirier, G. E. *Chem. Rev.* **1997**, *97*, 1117–1127, and references therein.
(15) Bumm, L. A.; Arnold, J. J.; Dunbar, T. D.; Allara, D. L.; Weiss, P. S. *J. Phys. Chem. B* In press.
(16) Allen, F. H.; Kennard, O.; Watson, D. G.; Brammer, L.; Orpen, A. G.; Taylor, R. *J. Chem. Soc., Perkin. Trans. 2* **1987**, S1–S19.
(17) Burkert, U.; Allinger, N. L. *Molecular Mechanics*, *ACS monograph*; American Chemical Society: Washington, D.C., 1982; Vol. 177.
(18) Dubois, L. H.; Nuzzo, R. G. *Annu. Rev. Phys. Chem.* **1992**, *43*, 437–463.
(19) Shi, J.; Hong, B.; Parikh, A. N.; Collins, R. W.; Allara, D. L. *Chem. Phys. Lett.* **1995**, *246*, 90–94.
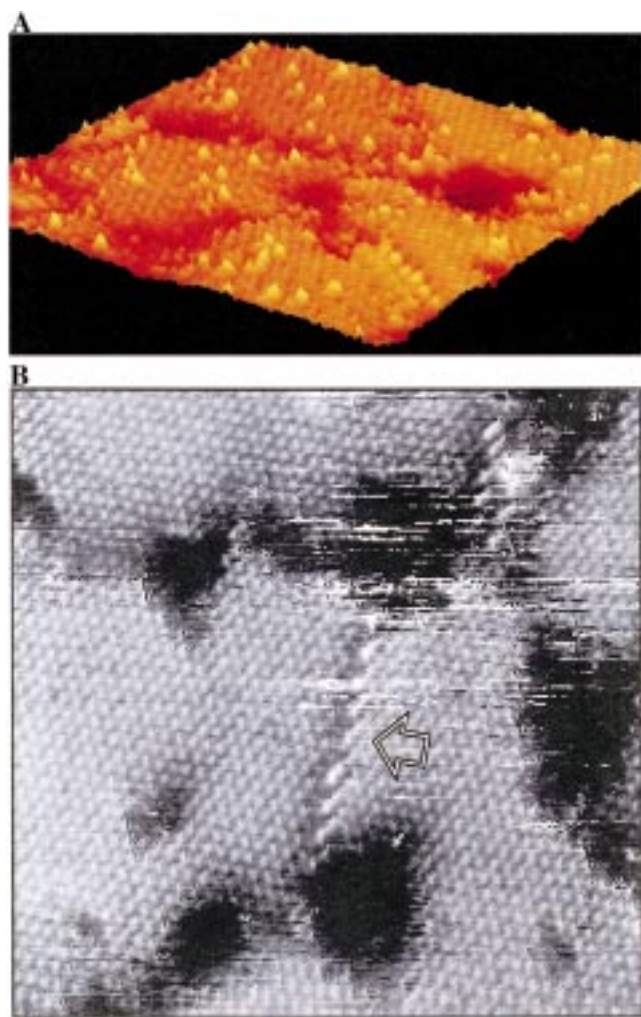
Figure 1. (A) Perspective view of the STM image of a coadsorbed mixed composition SAM of 95% **10**/5% **12**. We assign the higher (bright) features to the molecules of **12** which extend beyond the outer surface of the monolayer of **10**. Compare this to (B) the STM image of a single-component SAM of **10**. Note the lack of bright features as seen in **A**. Common features are the following: (1) the lower (shown as darker) spots are Au substrate vacancy islands (one atom deep holes in the underlying Au{111} substrate); (2) the alkanethiolate molecular lattice; (3) alkanethiolate structural domain boundaries; and (4) occasional higher features at domain boundaries (arrow) are due to a particular type of domain boundary. The images are of 250 Å × 250 Å areas and were recorded with a tip bias of +1.0 V and a tunneling current of 10 pA.

tilts and film structures when self-assembled on Au {111}.[18]) Note that **12** can be described as ω-ethyl-terminated **10**.

Results and Discussion

Coadsorbed Monolayers. We prepared a two-component SAM by coadsorption from a 95%/5% mixed solution of the thiols of **10** and **12**, respectively. As a control, single-component SAMs were also made from 100% **10** and 100% **12** using the identical procedure.

These alkanethiols on Au{111} are known to form domains of ($\sqrt{3} \times \sqrt{3}$) R30° and related superstructures.[14] Figure 1A is a STM topograph of the two-component SAM. The bright features in registry with the alkanethiolate lattice in Figure 1A correspond to the longer **12** molecules, which extend beyond the surface formed by the **10** component of the film. Similar results have been obtained using other length alkanethiol

combinations and component ratios.[20] Statistical analysis of the spatial distribution of **12** molecules shows that they are randomly distributed in the SAM and that they comprise ~5% of the SAM. For comparison, a single-component monolayer of **10** is shown in Figure 1B; similar results were obtained for a single-component SAM of **12**. Note that in Figure 1B all of the component molecules appear of similar height, although some of the alkanethiolate domain boundaries exhibit molecular features that appear higher than their neighbors (arrow). The identification of these domain boundaries has been discussed in ref 14. These are distinctly different from the two-component SAMs where well-defined higher features appear *within* the domains. Note that most domain boundaries are manifested by depressions.[14] The roughly circular depressions are Au substrate vacancy islands: one-Au-atomic-layer-deep pits in the substrate which are characteristic of room temperature self-assembly.[14,21,22]

We have used STM to measure the height difference between the **12** molecules and the surrounding **10** film. Because the **12** molecules protrude sharply from the film, the results are dependent on the characteristics of the STM probe tip. Furthermore the measured height of a protrusion (**12**) on a plane (**10** film) is dependent on the choice of measurement points due to their geometric dissimilarity. The molecular terraces described later in this paper provide a means for more precise determination of the topographic height differences. The topographic measurements can readily be made between two planes (a molecular terrace of **10** and one of **12**). These measurements and their interpretation are the subject of a forthcoming paper.[15]

High-Temperature Solution Processed Monolayers. We have investigated how SAMs can be modified using different processing conditions. A single-component SAM of **12** was heated for 1 h in a 1 mM solution of the thiol of **12** in ethanol at 78 °C. The result, shown in Figure 2A, was a dramatic decrease in the density of the structural domain boundaries and the Au substrate vacancy islands (cf. Figure 2B of ref 23, which shows an area of the same size). The size of the domains can be better appreciated from Figure 2B (this paper). Previously reported annealing procedures have not achieved this level of defect removal.[11,14,24–28] Dry annealing of SAMs can increase the coherence length of the SAM to >1000 Å, but the accompanying thiolate desorption generates defects within domains.[28] By annealing the SAM in the presence of excess thiol in solution, we have overcome this deficiency. In this way, the structural domains can be made so large as to be limited only by the size of the terraces of the underlying substrate. This is important in applications where chemical protection of the

(20) Charles, L. F.; Bumm, L. A.; Arnold, J. J.; Dunbar, T. D.; Allara, D. L.; Weiss, P. S., manuscript in preparation.

(21) Sondag-Huethorst, J. A. M.; Schönenberger, C.; Fokkink, L. G. J. *J. Phys. Chem.* **1994**, *98*, 6827−6833. *Ibid.* **1995**, *99*, 469−474.

(22) McDermott, C. A.; McDermott, M. T.; Green, J.-B.; Porter, M. D. *J. Chem. Phys.* **1995**, *99*, 13257−13267.

(23) Bumm, L. A.; Arnold, J. J.; Cygan, M. T.; Dunbar, T. D.; Burgin, T. P.; Jones, L., II; Allara, D. L.; Weiss, P. S. *Science* **1996**, *271*, 1705−1707.

(24) Schönenberger, C.; Jorritsma, J.; Sondag-Huethorst, J. A. M.; Fokkink, L. G. J. *J. Phys. Chem.* **1995**, *99*, 3259−3271.

(25) Delamarche, E.; Michel, B.; Kang, H.; Gerber, Ch. *Langmuir* **1994**, *10*, 4103−4108.

(26) McCarley, R. L.; Dunaway, D. J.; Willicut, R. J. *Langmuir* **1993**, *9*, 2775−2777.

(27) Bucher, J.-P.; Santesson, L.; Kern, K. *Langmuir* **1994**, *10*, 979−983.

(28) Camillone, N., III; Eisenberger, P.; Leung, T. Y. B.; Schwartz, P.; Scoles, G.; Poirier, G. E.; Tarlov, M. J. *J. Chem. Phys.* **1994**, *101*, 11031−11036.
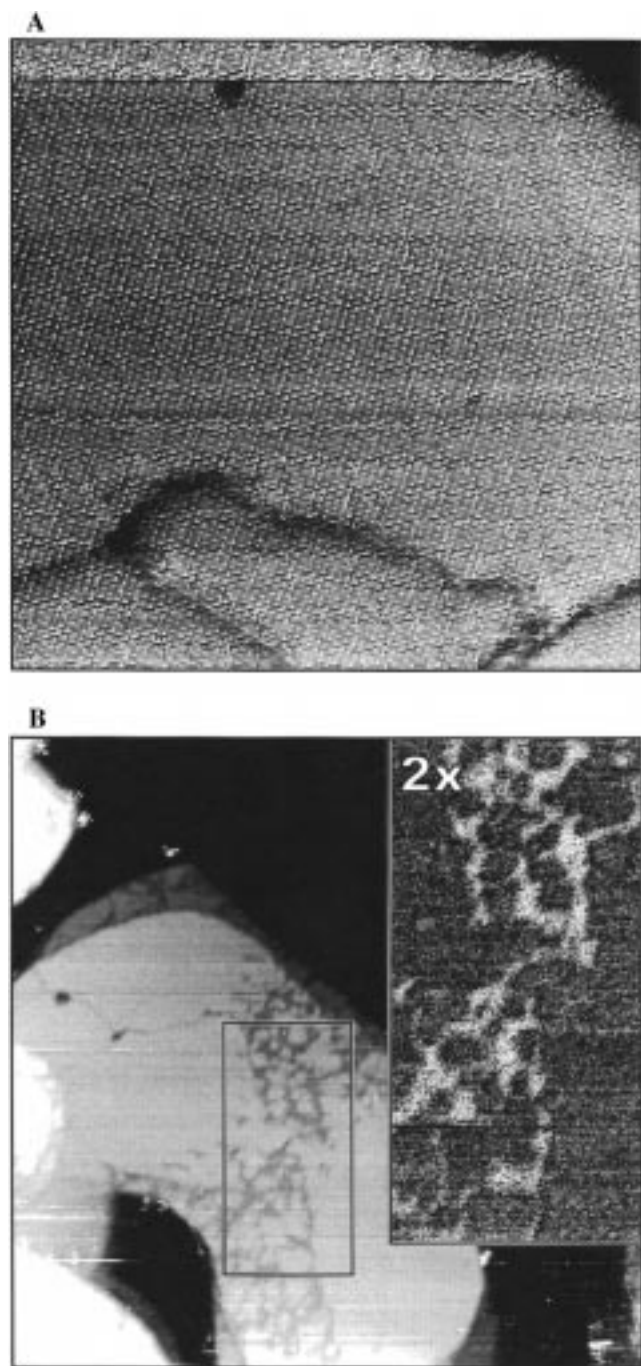
Figure 2. STM images of modified SAMs of **12** recorded with a tip bias of +1.0 V and a tunneling current of 10 pA. (A) An image of a 400 Å × 400 Å area of a SAM of **12** heated for 1 h in 1 mM thiol of **12** in ethanol at 78 °C showing that this treatment greatly reduces the defect density. (B) An image of a 5000 Å × 5000 Å area of a SAM of **12** heated for 1 h in neat ethanol at 78 °C showing both reduced defect density and partial monolayer desorption. The inset is an apparent tunneling barrier height image (2× greater magnification) acquired over the area delineated by the rectangle. Note that lower thiolate coverages *increase* the apparent tunneling barrier height.

substrate is required (e.g. corrosion resistance,[29] and resists for nanolithography[30]), or where highly uniform electronically insulating properties of the film are needed (e.g. blocking layers

for electrochemistry,[31] and defect-free dielectrics for micro-electronics[1]).[32]

Several mechanisms may contribute in this annealing process. Desorption of the thiolate is significant above 60 °C.[33] Infrared reflectance absorption spectroscopy indicates that the alkyl chain gauche fraction increases dramatically above room temperature.[18] X-ray diffraction studies of **10** SAMs in vacuo reveal that the onset of melting (softening and disorder) is coverage-dependent, ranging from 100 °C for full monolayers down to 20 °C for 50% coverage.[34] Disorder in the monolayer is expected to enhance exchange through greater access of the solution to the Au substrate and accelerated alkanethiolate desorption. Solvation of the thiolate and thiolate-Au species is also possible. Elevated temperatures increase the surface diffusion of both the alkanethiolate and the Au substrate.[11,24–27] Heating in the thiol solution allows Ostwald ripening of the SAM domains both by desorption/adsorption and by diffusion.

A STM image of a single-component SAM of **12**, heated for 1 h in neat ethanol at 78 °C, is shown in Figure 2B. Like the SAM heated in the thiol solution, the density of structural domain boundaries and the Au substrate vacancy islands has also decreased dramatically, so that the terrace is composed of only 3–4 large domains. A new structure has also formed wherein the monolayer breaks up, suffused by new features which appear lower and without molecular resolution. The transition between these regions occurs gradually. The observed height differences are not characteristic, nor do they correspond to typical features, namely, substrate steps (2.4 Å) or the film thickness of **12** (16 Å). We attribute these new features to partial desorption of the monolayer of **12**. The molecular lattice can still be resolved within the full monolayer domains but is not observed in these lower areas. This is consistent with X-ray diffraction studies which show that partial monolayers can have both regions of ordered c(4×2) and regions of a disordered intermediate phase.[34] In this intermediate phase we expect that the alkyl chains of a partial monolayer of **12** will be in a disordered and/or fluctuant state and hence not imaged by a room temperature STM.[35] An apparent tunneling barrier height (ATBH) image (inset) recorded of this area (rectangle) shows that the ATBH is greater over the lower area relative to the surrounding region, confirming that this is not a Au substrate feature.[36–39] The ATBH image also shows no contrast due to Au step edges (not shown). We attribute the ATBH contrast to

(29) Jennings, G. K.; Laibinis, P. E. *Colloids Surf. A* **1996**, *116*, 105–114.

(30) Seshadri, K.; Froyd, K.; Parikh, A. N.; Allara, D. L.; Lercel, M. J.; Craighead, H. G. *J. Phys. Chem.* **1996**, *100*, 15900–15909.

(31) Finklea, H. O. In *Electroanalytical Chemistry: A Series of Advances*; Bard, A. J., Rubinstein, I., Eds.; Marcel Dekker: New York, 1996; Vol. 19, pp 109–335.

(32) No lattice match is possible which crosses the boundaries imposed by substrate steps (Krom, K. R. Ph.D. Thesis, The Pennsylvania State University, University Park, PA, 1997).

(33) Finklea, H. O.; Ravenscroft, M. S.; Snider, D. A. *Langmuir* **1993**, *9*, 223–227.

(34) Schreiber, F.; Eberhardt, A.; Leung, T. Y. B.; Schwartz, P.; Wetterer, S. M.; Lavrich, D. J.; Berman, L.; Fenter, P.; Eisenberger, P.; Scoles, G. *Phys. Rev. B* **1998**, *57*, 12476–12481.

(35) Poirier, G. E.; Pylant, E. D. *Science* **1996**, *272*, 1145–1148.

(36) Weisendanger, R. *Scanning Probe Microscopy and Spectroscopy*; Cambridge University Press: New York, 1994.

(37) Chen, C. J. *Introduction to Scanning Tunneling Microscopy*; Oxford University Press: New York, 1993.

(38) Olesen, L.; Brandbyge, M.; Sørensen, M. R.; Jacobsen, K. W.; Lægsgaard, E.; Stensgaard, I.; Besenbacher. F. *Phys. Rev. Lett.* **1996**, *76*, 1485–1488.

(39) The ATBH is related to the local work function.[36–38] The dipole-layer model predicts that the work function will increase with increasing thiolate coverage (Somorjai, G. A. *Introduction to Surface Chemistry and Catalysis*; J. Wiley: New York, 1994.); however experiments show that adsorption of alkanethiolates *decreases* the work function (Evans, S. D.; Urankar, E.; Ulman, A.; Ferris, N. *J. Am. Chem. Soc.* **1991**, *113*, 3, 4121–4131). In this work we use ATBH images as a qualitative tool to demonstrate that these two regions of the SAM differ by more than just their height.

the different alkanethiolate coverages and to the different functional groups exposed at the film exterior. Whereas only ordered methyl groups are exposed in the crystalline domains, both methyl and methylene groups should be exposed in the disordered liquidlike regions.

An image of a single-component SAM of **12**, partially desorbed as in Figure 2B and subsequently immersed into a 1 mM solution of **10** in ethanol at room temperature for 6 h, is shown in Figure 3A. Domains of **12** are present largely as well ordered islands—remnants of the treatment in hot ethanol which dramatically reduces the defect density. The islands of **12** are surrounded by **10**, displaying defect densities typical of SAMs formed at room temperature. A slight intermixing of the components can also be observed in Figure 3A, where isolated molecules of **12** occur in domains of **10** and vice versa.

The boundaries between the islands of **12** and the surrounding **10** are molecularly sharp, as shown in Figure 3B. Note that there may be alkanethiolate lattice registry between the molecular terraces of **10** and **12**, yielding what we term "lateral epitaxy." That is, the lattice of one molecule is grafted onto the lattice of the other without *physical* defects. Compare the **10/12** island boundaries (**a** and **b**) to the **10/10** structural domain boundaries (**c**) in Figure 3, parts A and B. The perturbation on the monolayer structure caused by the latter extends over 2−3 nearest-neighbor spacings. By contrast the alkanethiolate lattice continues uninterrupted across some of the **10/12** island boundaries (**a**) in Figure 3A while others (**b**) are clearly associated with **10/10** structural domain boundaries.

Our ability to prepare these molecular terraces allows us to access a new regime in molecular engineering. At the epitaxial boundaries between the molecular terraces, the chains of the longer molecules are exposed. The greater access to the molecules (reduced steric hindrance by the surrounding monolayer) at these boundaries will increase the chemical reactivity of the exposed functional groups. Thus the film structure can be used to direct surface chemistry. In addition, controlling the exposed functionality at the outside of each molecular terrace, we may vary the relative surface energies of the steps at the boundaries vs atop the terraces in a way that is not possible for simple crystalline surfaces. We intend to use these structures of uniquely exposed functionality to direct reactions selectively to these topologically one-dimensional sites.[40] This is analogous to the observed special reactivity of atomic steps on single-crystal metal surfaces.[41−44]

The molecularly sharp **10/12** boundaries (Figures 3A and 3B) are stable at room temperature in air and dry nitrogen. The area in Figure 3A was imaged for over 1 h, and during that time, no motion of the molecular components within the densely packed domains was observed (see also the image of an overlapping area imaged 1 h later, Figure 1A of ref 15). In Figures 1A and 3A the isolated molecules of **12** in the domains of **10** (and vice versa) serve as markers for intradomain diffusion, but no such motion is observed. We have observed the apparent switching of rows of molecules between structural domains, but this does not necessitate motion of the sulfur headgroups. The prominent feature at the edge of the Au substrate vacancy island does not
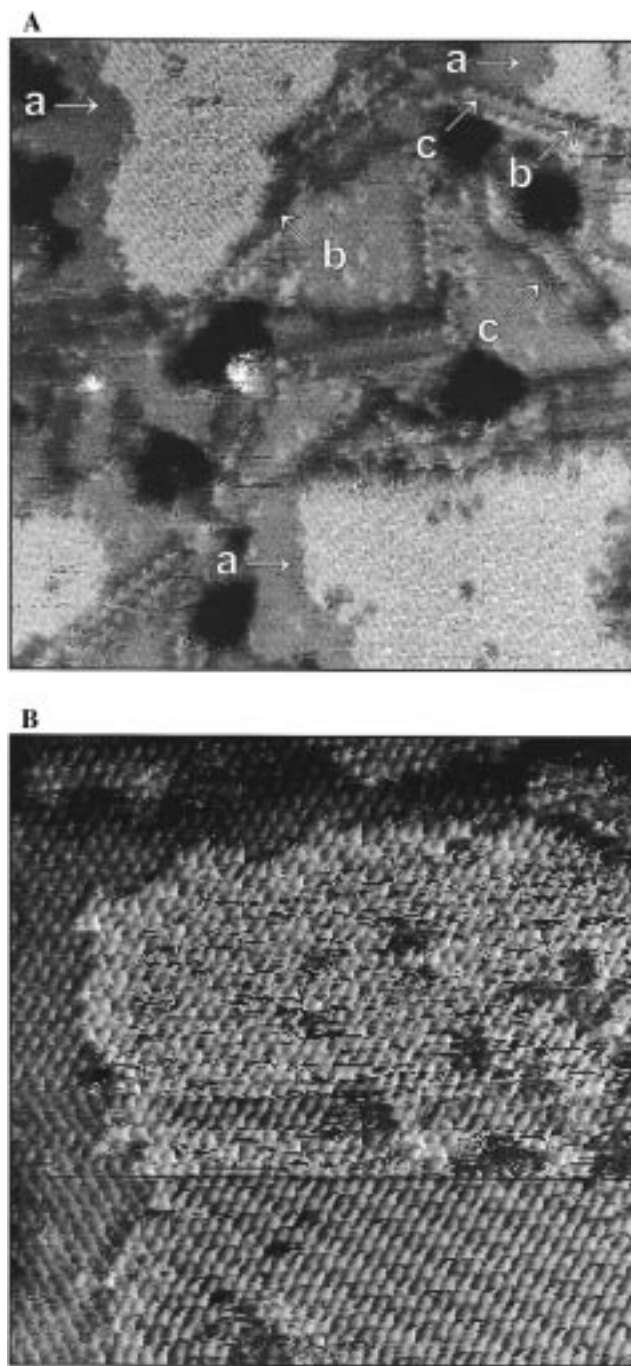
(40) Weiss, P. S.; Yokota, H.; Aebersold, R.; van den Engh, G.; Bumm, L. A.; Arnold, J. J.; Dunbar, T. D.; Allara, D. L. *J. Phys.: Condens. Matter* **1998**, *10*, 7703−7712.

(41) Henderson, M. A.; Szabo, A.; Yates, J. T., Jr. *J. Chem. Phys.* **1989**, *91*, 7255−7264.

(42) Weiss, P. S.; Eigler, D. M. *Phys. Rev. Lett.* **1992**, *69*, 2240−2243.

(43) Stranick, S. J.; Kamna, M. M.; Weiss, P. S. *Science* **1994**, *266*, 99−101.

(44) Zambelli, T.; Wintterlin, J.; Trost, J.; Ertl, G. *Science* **1996**, *273*, 1688−1690.

Figure 3. A partially desorbed SAM of **12** prepared as in Figure 2B was subsequently immersed in a 1 mM solution of a shorter chain thiol (10) for 6 h at room temperature. (A) This results in domains of **12**, remnants of the hot ethanol treatment, and a surrounding monolayer of 10, characteristic of room temperature self-assembly. This 500 Å × 500 Å area image was recorded with a tip bias of +1.0 V and a tunneling current of 5 pA. The arrows identify examples of three types of SAM boundaries: (a) 10/12 laterally epitaxial boundaries and (b) 10/12 boundaries associated with (c) 10/10 structural domain boundaries. (B) Molecularly sharp boundaries are observed at the edges of the domains of 12. This 250 Å × 250 Å area image was recorded with a tip bias of +1.0 V and a tunneling current 10 pA.

move within the film but does change its apparent height in STM images, visible at the left of the image center in Figure 3A (this paper) and at the lower left in Figure 1A of ref 15. Fully conjugated guest molecules inserted into the boundaries described in ref 23 were observed for hours without motion. The room temperature stability of the molecularly sharp island

boundaries is significant in our ability to create molecular- and nanometer-scale structures.

Despite the fact that STM is routinely used to image molecules and molecular assemblies, which are insulators in the bulk, the mechanism by which electrons tunnel through molecular frameworks remains poorly understood.[15] This has lead some investigators to propose that "the alkyl chains contribute minimally to the tunneling, if at all"[35] and to attribute the observed resolution of the molecular lattice to the sulfur headgroups alone.[24] However the results in Figures 1A and 3 cannot be reconciled with this view. If the chains did not contribute to the electron tunneling, the height differences between **10** and **12** would not be detected. Additionally, alkanethiolate SAMs with a 10−12 carbon backbone must be imaged at high tunnel junction transimpedance, $Z \gtrsim 100$ GΩ, in order for the monolayer not to be perturbed by the tip (high tunnel junction transimpedance corresponds to large tip−sample separations). When a SAM is imaged at significantly lower Z, subsequent imaging at high Z reveals that the structure of the monolayer has been perturbed.[21] We conclude that the chains must participate in electron tunneling. In a forthcoming paper, we quantify the difference between the electron tunneling through **10** and **12** and show that it is consistent with the known behavior of electron transfer through σ-bonded hydrocarbon chains.[15]

Conclusions

We have demonstrated that stable, two-component, monolayers films with molecularly sharp boundaries can be synthesized and that the placement of the two molecules within the film can be controlled by selecting deposition and processing strategies. The adsorbate structural domains can be made so large as to be limited by the underlying terrace size of the substrate. We are now using these structures to study the surface chemistry of organic monolayer films and as model systems to study electron transfer through molecular frameworks.[15,23,45]

Experimental Section

Au{111} Substrate Preparation. Oriented thin-film Au{111} substrates were prepared using a procedure developed by Chidsey et al.[46] They were prepared by depositing 120 nm of 99.999% pure Au[47] at 0.1 nm/s onto freshly cleaved muscovite mica[48] in vacuo with a base pressure $< 5 \times 10^{-7}$ Torr. The mica substrate had been ramped from room temperature to 340 °C at the rate of 32 °C/h and held at the deposition temperature for 18 h prior to, during, and 1 h after deposition. The Au films were allowed to cool to <30 °C in a vacuum for 18 h.

Alkanethiols. The 1-alkanethiols, 1-decanethiol and 1-dodecanethiol, were obtained from Aldrich,[49] purified by vacuum distillation, and stored at −20 °C until use.

Monolayer Preparation. Films were prepared by self-assembly of **10**, **12**, or mixtures from solutions that were 1 mM in total alkanethiol in ethanol. The substrate was immersed in the alkanethiol solution for 18−24 h. The SAMs were rinsed sequentially in hexane, acetone, and ethanol and then blown dry with purified N_2.

High-Temperature Solution Processing. The temperature was rapidly increased by inserting the container with the solution-immersed SAM into a 78 °C bath. Rapid quenching was achieved by cooling the container in cold running water, followed immediately by rinsing the SAM sample 10 times in absolute ethanol and blowing it dry.

The Scanning Tunneling Microscope. We use a beetle-style scanning tunneling microscope,[50,51] which has been specially constructed so that tunnel junction bias frequencies from DC to 20 GHz can be applied to the tunnel junction by means of a tunneling tip that is part of and fed by a coaxial transmission line.[52−54] Controlled geometry Pt/Ir tips were used as the scanning probes.[55] The tunneling current is detected using an Axon CV4 patch clamp transimpedance amplifier,[56,57] which enables us to acquire STM images at tunnel currents as low as 0.1 pA with a 2.1 kHz bandwidth.[58] The microscope was enclosed in a controlled atmosphere using a constant dry N_2 purge.

Lattice-Resolved Imaging. All SAMs were imaged using the scanning tunneling microscope in constant current feedback (topographic mode).[36,37] Our images were acquired with a tunnel junction transimpedance of 100 GΩ or greater in order to ensure that the probe tip does not come into contact with the film.[15] Apparent tunneling barrier height images were acquired simultaneously with topographic images by applying a 5 kHz ∼0.1 Å peak-to-peak sinusoidal modulation to the tip−sample separation while maintaining constant current feedback control (bandwidth DC to 2.1 kHz, limited by a 4-pole low-pass Bessel filter). A Stanford Research model 850 lock-in amplifier[59] at a bandwidth of 100 Hz was used to measure the 5 kHz ATBH component of the tunneling current on the unfiltered output of the transimpedance amplifier (bandwidth DC to 30 kHz). The STM images shown are not filtered.

Supporting Information Available: A gray scale image of the perspective view shown in Figure 1A. This material is available free of charge via the Internet at http://pubs.acs.org.

JA982157L

(45) Cygan, M. T.; Dunbar, T. D.; Arnold, J. J.; Bumm, L. A.; Shedlock, N. F.; Burgin, T. P.; Jones, L., II; Allara, D. L.; Tour, J. M.; Weiss P. S. *J. Am. Chem. Soc.* **1998**, *120*, 2721−2732.

(46) Chidsey, C. E. D.; Loiacono, D. N.; Sleator, T.; Nakahara, S. *Surf. Sci.* **1988**, *200*, 45−66.

(47) Refining Systems, P.O. Box 72466, Las Vegas, NV 89170.

(48) Asheville-Schoonmaker Mica Co., 900 Jefferson Ave., P.O. Box 318, Newport News, VA 23607.

(49) Aldrich, 1001 W. St. Paul Ave., Milwaukee, WI 53233 (http://www.sial.com/).

(50) Besocke, K. *Surf. Sci.* **1987**, *181*, 145−153.

(51) Frohn, J.; Wolf, J. F.; Besocke, K.; Teske, M. *Rev. Sci. Instrum.* **1989**, *60*, 1200−1201.

(52) Stranick, S. J.; Weiss, P. S. *Rev. Sci. Instrum.* **1993**, *64*, 1232−1234.

(53) Stranick, S. J.; Weiss, P. S. *Rev. Sci. Instrum.* **1994**, *65*, 918−921.

(54) Bumm, L. A.; Weiss, P. S. *Rev. Sci. Instrum.* **1995**, *66*, 4140−4145.

(55) Materials Analytical Services, Inc., 616 Hutton St., Suite 101, Raleigh, NC 27606.

(56) Axon Instruments Inc., 1101 Chess Dr., Foster City, CA 94404 (http://www.axonet.com/).

(57) Dunlop, D.; Smith, S.; Bustamante, C.; Tamayo, J.; Garcia, R. *Rev. Sci. Instrum.* **1995**, *66*, 4876−4879.

(58) We have limited the bandwidth of the CV4 signal used of STM feedback control with a 4-pole low-pass Bessel filter. This gives us an excellent signal-to-noise for current feedback and also the ability to simultaneously use the frequencies above this band for other measurements.

(59) Stanford Research Systems, 1290 D Reamwood Ave., Sunnyvale, CA 94089 (http://www.srsys.com/srsys/).